

Structure and stability of Ba-Cu-Ge type-I clathrates

Yang Li, Ji Chi, Weiping Gou, Sameer Khandekar, and Ross, Jr., Joseph H.
Department of Physics, Texas A&M University, College Station, TX 77843-4242

(Dated: February 7, 2020)

We have prepared samples of nominal type $\text{Ba}_8\text{Cu}_x\text{Ge}_{46-x}$ by induction melting and solid state reaction. Analysis has shown that these materials form type-I clathrates, with copper content between $x = 4.6$ and 5.2 , nearly independent of the starting composition. X-ray powder diffraction and single-crystal electron diffraction results confirmed the cubic type-I clathrate structure to be the main phase in these materials. For starting compositions of $\text{Ba}_8\text{Cu}_2\text{Ge}_{44}$ and $\text{Ba}_8\text{Cu}_4\text{Ge}_{42}$, electron microprobe analysis demonstrated the formation of clathrate with average composition $\text{Ba}_{7.8}\text{Cu}_{4.7}\text{Ge}_{39.3}$, along with elemental Ge and a small amount of BaGeO_2 . In a $\text{Ba}_8\text{Cu}_6\text{Ge}_{40}$ preparation, Cu content of the clathrate phase increased to $x = 5.1$, while excess Cu appeared as a Ge_3Cu_5 phase. The stability of the $x \approx 5$ composition in $\text{Ba}_8\text{Cu}_x\text{Ge}_{46-x}$ we attribute to an electron magic-number mechanism, associated with a gap or deep minimum in the Fermi-level density of states. Indeed, electrical transport measurements indicated the Cu_4 and Cu_6 samples to have a temperature dependence indicative of semiconducting or semimetallic behavior.

I. INTRODUCTION

Silicon, germanium, and tin form clathrate phases having framework structures in which the cages generally enclose single ions of the alkali metal, alkali earth, rare earth or halogen series.^{1,2,3} Doping with metal atoms has led to a wide variety of electronic behavior, including superconductivity in $\text{Ba}_8\text{Si}_{46}$,⁴ and in $\text{Ba}_8\text{Ga}_{16}\text{Ge}_{30}$,⁵ ferromagnetism in $\text{Ba}_8\text{Mn}_2\text{Ge}_{44}$,⁶ and a number of semiconducting compositions including the silicon-only material Si_{136} .⁷ There has been considerable interest in these materials, for a number of potential applications including thermoelectric cooling.^{2,3,8} There is the further potential for epitaxial growth in conventional semiconductor systems,⁹ and transition-metal and rare-earth-doped clathrates offer the possibility of new magnetic semiconductors.

We have studied the formation of Ba-Cu-Ge clathrates, and report on the stable formation of clathrates with the type-I structure and compositions close to $\text{Ba}_8\text{Cu}_5\text{Ge}_{39}$. This composition forms preferentially for a range of starting compositions, for ambient-pressure synthesis. The formation of Ba-Cu-Ge type-I clathrates has been reported previously.¹⁰ It is known that Cu substitutes for Ge on framework sites, although the nearness of Cu and Ge in the periodic table makes identification of specific Cu atomic positions via x-ray Rietveld analysis somewhat difficult.

In type-I germanium-barium clathrates, of nominal composition $\text{Ba}_8\text{Ge}_{46}$, germanium occupies three sites, which are Wyckhoff $6c$, $16i$, and $24k$ sites in the cubic $\text{Pm}\bar{3}\text{n}$ (#223) structure. This structure is the analog of the $(\text{Cl}_2)_8(\text{H}_2\text{O})_{46}$ gas clathrate.² Ba ions occupy $2a$ and $6d$ sites, corresponding to locations within the two distinct cages of the Ge framework. By analogy with the tin clathrates,¹¹ the stable semiconducting composition would be expected to be $\text{Ba}_8\text{Ge}_{42}$, with vacancies preferentially appearing at $6c$ sites, while experimentally the $\text{Ba}_8\text{Ge}_{43}$ composition has been reported.¹² A number of transition metals have been incorporated into this

structure,¹⁰ predominantly by substitution for Ge at the $6c$ site. The preference for this site can be understood in terms of the reduced electron density appearing at this site.

Based on recent work on Au-doped Ge clathrates¹² and noble-metal-doped Si clathrates,^{13,14} we expected to find Cu-doping for a range of compositions in Ba-Ge clathrates. However, electron microprobe analysis showed that Cu prefers to substitute in a relatively narrow range of composition, as detailed below. In the Analysis and Discussion section we describe a relatively simple electron counting argument that explains this result, while electrical transport measurements also support this conclusion.

II. EXPERIMENT

Ingots with nominal compositions $\text{Ba}_8\text{Cu}_x\text{Ge}_{46-x}$, for $x = 2, 4$ and 6 , were formed by rf induction melting and solid-state reaction. These samples will be referred to as samples Cu2, Cu4, and Cu6, respectively. Stoichiometric quantities of the elemental materials were finely powdered and pressed into BN crucibles, then induction heated in an argon atmosphere. The resulting ingots, exhibiting a metallic luster, were further reacted at 950°C for 3 days followed by 700°C for 4 days, in evacuated ampoules.

Analysis by Cu $K\alpha$ powder x-ray diffraction showed these ingots to consist mainly of the cubic type-I clathrate, plus small amounts of diamond-structure Ge in the Cu2 and Cu4 samples. While the x-ray samples were taken from the central portion of each ingot, WDS measurements described below indicate that the clathrate formed toward the center of the ingots, with additional Ge remaining at the periphery of these ingots. LeBail extraction and Rietveld refinement were performed using GSAS software,^{15,16} giving lattice parameters of 1.0693 nm for the Cu2 sample, 1.0686 nm for Cu4, and 1.0680 nm for Cu6. These values are compa-

TABLE I: The measured parameters for the three samples obtained from powder x-ray diffraction, and the bond lengths calculated using these atomic positions.

Sample	Cu2	Cu4	Cu6
a (nm)	1.0693	1.0686	1.0680
x	0.181	0.183	0.184
y	0.314	0.316	0.311
z	0.121	0.119	0.119
Ba $2a$ occupancy	0.91	0.90	0.73
Ba $6d$ occupancy	1.00	1.00	1.00
$6c - 24k$ (nm)	0.242	0.241	0.246
$16i - 16i$ (nm)	0.257	0.248	0.246
$16i - 24k$ (nm)	0.248	0.251	0.248
$24k - 24k$ (nm)	0.259	0.254	0.254

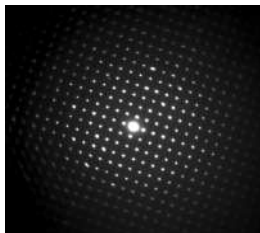


FIG. 1: Electron diffraction pattern obtained for the Cu6 sample, showing a cubic pattern characteristic of the type-I clathrate.

table to the value previously reported¹⁰ for a sample of composition $\text{Ba}_8\text{Cu}_6\text{Ge}_{40}$, 1.06859 nm. Our x-ray results are summarized in Table I.

A scanning electron microscopy analysis showed that in the Cu2 and Cu6 samples, the ingots consist of large clathrate crystallites of several-100 μm , with smaller crystallites of other phases. A powdered specimen from the Cu6 ingot placed on a grid for transmission-electron microscopy showed the characteristic cubic diffraction pattern (Fig. 1). Electron diffraction images from several crystallites in this sample were compared to simulations obtained using MacTempas software,¹⁷ giving a good match to the observations, with no superlattice structure observed. A superlattice was previously observed in $\text{Ba}_8\text{Ge}_{43}$, indicating an ordered configuration for the apparently 3 framework vacancies per cell.¹² As shown below, our samples contain somewhat fewer vacancies, and apparently these are randomly distributed.

In the Rietveld refinement process, fits of equivalent goodness were obtained for a range of Cu atom locations and relative occupations. This insensitivity to Cu occupation is due to the nearness of Cu and Ge in the periodic table. However, these fits showed that the relatively few Ba vacancies appear preferentially on the $2a$ sites, located in the smaller of the two cages. The relative occupations of the two Ba sites are given in Table I. The analysis further indicated the clear presence of Ge/Cu vacancies on the $6c$ site, although it was difficult to obtain the relative numbers of these atoms. Fig. 2 shows an x-ray diffrac-

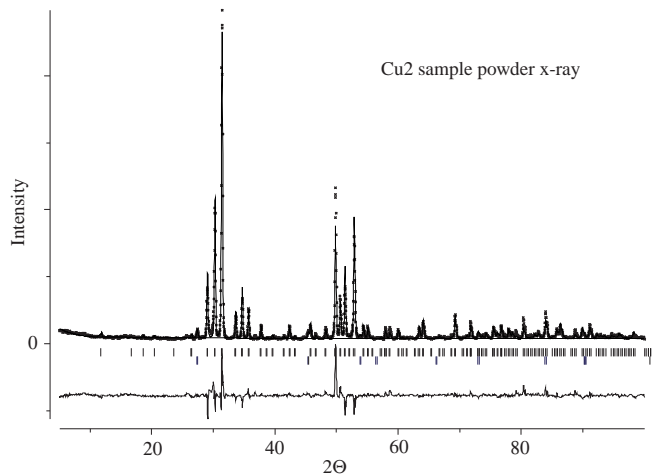


FIG. 2: Cu K- α powder x-ray diffraction pattern for the sample of nominal composition $\text{Ba}_8\text{Cu}_2\text{Ge}_{44}$. A fit to the type-I clathrate structure is superposed on the data, with the difference plot given below. Vertical bars indicate the reflections identified in the fit, with the upper set corresponding to the type-I clathrate structure, and the lower set corresponding to Ge.

TABLE II: Parameters derived from WDS microprobe results.

Sample	Cu2	Cu4	Cu6
Ba/cell	7.8	7.8	7.5
Cu/cell	4.8	4.6	5.1
Ge/cell	39.8	38.8	39.1

tion pattern from the Cu2 sample, with a fit showing the well-formed type-I clathrate structure in this material.

For the $\text{Pm}\bar{3}\text{n}$ (#223) structure, the $6c$ site has position $(1/4, 0, 1/2)$, while the $16i$ position is given by (x, x, x) , and the $24k$ position, $(0, y, z)$. The parameters x , y , and z are given in Table I as obtained in the refinement. Also given in the table are the bond lengths separating Ge sites, as extracted from these parameters.

Further analysis of these samples was carried out using a commercial wavelength dispersive spectroscopy (WDS)-based electron microprobe apparatus and analysis system.¹⁸ From these measurements an abundant clathrate phase was identified in each sample, for which the atomic occupancies are displayed in Table II, normalized to reflect the number of atoms per cubic cell. Both Rietveld x-ray analysis and the WDS analysis provide a relative number of atoms per cell, rather than an absolute composition. For the results displayed in Table II, we normalized the results according to the relative Ba occupation on the $2a$ site, as found by x-ray diffraction (Table I), assuming the Ba $6d$ site to be fully occupied. These atomic occupations correspond to Ba vacancies between 0.2 and 0.5 per cell, and framework vacancies (Ge + Cu) between 1.4 and 2.6 per cell.

While there are small differences in the atomic occupations for the Cu2 and Cu4 samples, the values are quite

close. For both of these samples, the Cu:Ge ratio exceeds that of the starting composition. Apparently a composition close to $\text{Ba}_8\text{Cu}_{4.7}\text{Ge}_{3.9}$ is favored under these preparation conditions. The minority phases observed in these two samples are pure Ge, and an oxide of approximate composition BaGeO_2 . Ge appeared as inclusions within the abundant clathrate phase, indicating a phase separation during the solid state reaction and annealing process. In one location an additional Ge-Ba-S phase was detected in the Cu4 sample, attributed to a localized impurity left after H_2SO_4 cleaning of the mortar and pestle, however no S was detected in any of the other analyses. The Ba-Ge oxide was not found to contain Cu in any of the samples.

Scans of the Cu6 were quite similar to those of the other two samples, however an additional minority phase was observed in this sample, of nominal composition $\text{GeCu}_{1.65}$, or Ge_3Cu_5 . This phase appeared to be in equilibrium with the clathrate and Ge phases (the latter containing about 1 at.% Cu). We deduce that the Cu content of the sample as prepared exceeded the stability limit for the clathrate, so that approximately 10% of the Cu appears as Ge_3Cu_5 (or about 2 at.% of the entire sample). However, the clathrate was driven to a slightly higher Cu content, and the Cu occupancy apparently scales with the first-neighbor bond lengths for the $6c$ site ($6c$ - $24k$ bond length, Table I).

The Ge_3Cu_5 is consistent with the observed x-ray spectrum indicating an essentially single-phase clathrate sample, since a minority phase of relative concentration 2% will not be obvious in the x-ray spectrum, particularly if the line positions are not known. Ge_3Cu_5 has not been previously reported to our knowledge,¹⁹ and may be a new intermetallic, possibly stabilized by the adjacent phases. None of the Ge-Cu intermetallic structures that have been reported, GeCu_3 , GeCu_5 , or Ge_2Cu_5 , could be identified in the x-ray diffraction spectrum for the Cu6 sample.

To further understand the electronic features of these materials, we measured the electrical resistivity on samples sliced from the Cu4 and Cu6 ingots. These ingots are easily fractured due to their inhomogeneous compositions, and they could not easily be cut into uniform bars. However, we obtained two samples of approximate dimension $1 \times 1 \times 1$ mm, and made four-probe measurements on these samples using silver-paint contacts.

Resistance results are shown in Fig. 3. The Cu4 dataset was obtained in an applied field of $H = 0.1$ T; the $H = 0$ result showed very similar features, but had instabilities we attributed to changes in contacts. In this case both samples were approximately the same size, which implies that the Cu4 resistivity is somewhat larger. However the temperature dependences are quite similar, changing from apparently semiconducting to metallic behavior at about 150 K. Our tentative conclusion from these data is that both materials are semimetals, with carrier localization becoming important at lower temperatures. The Cu6 data show two peaks at lower temper-

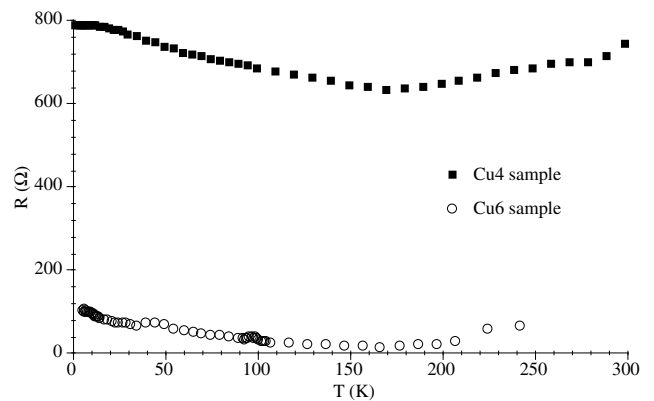


FIG. 3: Electrical resistance for the Cu4 and Cu6 samples vs. temperature. Applied field is 0.1 T for the upper curve, as described in the text.

atures, which correspond to weak magnetic transitions which we are now further investigating. In the vicinity of these peaks, it is possible to fit the data to activated behavior (e^{-T/T_0}) or variable-range hopping behavior ($e^{T^{-1/4}}$), without sufficient baseline to distinguish these behaviors.

III. ANALYSIS AND DISCUSSION

One expects the hypothetical type-I clathrate Ge_{46} to be a semiconductor, based on the results of LDA electronic-structure calculations.²⁰ This holds as well for Sn and Si clathrates.^{11,21} For the case of Sn clathrates, the stable phase $\text{Cs}_8\text{Sn}_{44}$ is also found theoretically to be semiconducting.¹¹ Presumably this stability can be attributed to the influence of a filled band, as the valence electrons of the two missing Sn atoms offset the eight electrons donated by Cs. Similar valence-counting arguments would also predict the stability of $\text{Cs}_8\text{Ga}_8\text{Sn}_{38}$ and $\text{Cs}_8\text{Zn}_4\text{Sn}_{42}$, which are also found theoretically to be semiconducting.¹¹ One assumes this strong stabilizing influence to be due to the prominent and relatively large energy gap in these semiconducting phases.

The ionic character of Ba in the clathrates is less clear than that of the alkali metals,^{21,22,23} due to mixing of the Ba $5d$ orbitals into the conduction band in the type-I clathrates. For example, a phase close to $\text{Ba}_8\text{Ge}_{43}$ in composition is observed to be stable,^{12,24} while valence-counting predicts $\text{Ba}_8\text{Ge}_{42}$ to be stable, assuming two electrons donated per Ba. If we assume Cu to have valence 1 and Ba valence 2, valence counting predicts the stable phase to be $\text{Ba}_8\text{Cu}_{(16/3)}\text{Ge}_{(46-16/3)} = \text{Ba}_8\text{Cu}_{(5.3)}\text{Ge}_{(40.7)}$. These values are quite close to the values observed in our measurements (Table II).

The valence-counting argument described here assumes that the number of electrons per cell corresponds to 92 filled bands, as in the hypothetical semiconductor Ge_{46} . A deep minimum in density of states at the Fermi

level, or perhaps semiconducting behavior, should then be expected for the most stable composition. The resistances observed for the Cu₄ and Cu₆ samples (Fig. 3) indeed are consistent with this, as described above. This provides further support for the existence of a gap or pseudogap in these materials. The fact that we do not observe complete filling of the Ba and framework sites, however, implies a deficit of electrons, and presumably the expulsion of a small number of bands into the conduction band due to hybridization of Ba and Cu *d* orbitals. This feature would explain the observation of weak magnetism, as described above.

IV. CONCLUSIONS

In conclusion, we have prepared type-I clathrates from different starting Ba-Cu-Ge compositions, and find there

to be a stable preferred composition for this material. WDS measurements supported by x-ray diffraction and electron diffraction measurements showed that the stable phase has a composition close to Ba_{7.7}Cu_{4.8}Ge_{39.2}. A simple valence-counting argument was found to account for the stability of this material, and electrical resistance measurements confirmed this composition to be semiconducting or semimetallic.

Acknowledgments

This work was supported by the Robert A. Welch Foundation, Grant No. A-1526.

-
- ¹ G. K. Ramachandran, J. J. Dong, J. Diefenbacher, J. Gryko, R. F. Marzke, O. F. Sankey, and P. F. McMillan, *J. Solid State Chem.* **145**, 716 (1999).
- ² G. S. Nolas, T. J. R. Weakley, J. L. Cohn, and R. Sharma, *Phys. Rev. B* **61**, 3845 (2000).
- ³ G. S. Nolas, B. C. Chakoumakos, B. Mahieu, G. J. Long, and T. J. R. Weakley, *Chem. Mater.* **12**, 1947 (2000).
- ⁴ S. Yamanaka, E. Enishi, and H. Fukuoka, *Inorg. Chem.* **39**, 56 (2000).
- ⁵ J. D. Bryan, *Phys. Rev. B* **60**, 3064 (1999).
- ⁶ T. Kawaguchi, K. Tanigaki, and M. Yasukawa, *Appl. Phys. Lett.* **77**, 3438 (2000).
- ⁷ J. Gryko, P. F. McMillan, and R. F. Marzke, *Phys. Rev. B* **62**, R7707 (2000).
- ⁸ J. L. Cohn, G. S. Nolas, V. Fessatidis, T. H. Metcalf, and G. A. Slack, *Phys. Rev. Lett.* **82**, 779 (1999).
- ⁹ S. Munetoh, K. Moriguchi, K. Kamei, A. Shintani, and T. Motooka, *Phys. Rev. Lett.* **86**, 4879 (2001).
- ¹⁰ G. Cordier and P. Woll, *J. Less-Common Met.* **169**, 291 (1991).
- ¹¹ C. W. Myles, J. Dong, and O. F. Sankey, *Phys. Rev. B* **64**, 165202 (2001).
- ¹² R. F. W. Herrmann, K. Tanigaki, T. Kawaguchi, S. Kuroshima, and O. Zhou, *Phys. Rev. B* **60**, 13245 (1999).
- ¹³ R. F. W. Herrmann, K. Tanigaki, S. Kuroshima, and H. Suematsu, *Chem. Phys. Lett.* **283**, 29 (1998).
- ¹⁴ Y. Nozue, G. Hosaka, E. Enishi, and S. Yamanaka, *Mol. Cryst. Liq. Cryst.* **341**, 509 (2000).
- ¹⁵ A. C. Larson and R. B. von Dreele, *Tech. Rep. LAUR 86-748*, Los Alamos National Laboratory (2000).
- ¹⁶ B. H. Toby, *J. Appl. Cryst.* **34**, 210 (2001).
- ¹⁷ *Mactempas software, total resolution, berkeley, ca.*
- ¹⁸ *Cameca instrument inc. sx-50.*
- ¹⁹ P. Villars and L. D. Calvert, *Pearson's handbook of crystallographic data for intermetallic phases* (ASM International, 1991).
- ²⁰ J. Zhao, A. Buldum, J. P. Lu, , and C. Y. Fong, *Phys. Rev. B* **60**, 14177 (1999).
- ²¹ S. Saito and A. Oshiyama, *Phys. Rev. B* **51**, 2628 (1995).
- ²² K. Moriguchi, S. Munetoh, and A. Shintani, *Phys. Rev. B* **62**, 7138 (2000).
- ²³ N. P. Blake, D. Bryan, S. Lattner, L. Mollnitz, G. D. Stucky, and H. Metiu, *J. Chem. Phys.* **114**, 10063 (2001).
- ²⁴ W. Carrillo-Cabrera, J. Curda, K. Peters, S. Paschen, M. Baenitz, Y. Grin, and H. G. von Schnering, *Z. Kristall.* **215**, 321 (2000).